



Published in final edited form as:

Langmuir. 2012 November 20; 28(46): 16115–16125. doi:10.1021/la302566p.

Glycosaminoglycan-Mediated Selective Changes in the Aggregation States, Zeta Potentials, and Intrinsic Stability of Liposomes

Erin K. Nyren-Erickson[†], Manas K. Haldar[†], Jessica R. Totzauer[§], Riley Ceglowski, Dilipkumar S. Patel[§], Daniel L. Friesner[§], D. K. Srivastava[‡], and Sanku Mallik^{*,†}

[†]Department of Pharmaceutical Sciences, North Dakota State University, Fargo, North Dakota 58108-6050

[§]Department of Pharmacy Practice, North Dakota State University, Fargo, North Dakota 58108-6050

[‡]Department of Chemistry and Biochemistry, North Dakota State University, Fargo, North Dakota 58108-6050

Abstract

Though the aggregation of glycosaminoglycans (GAGs) in the presence of liposomes and divalent cations has been previously reported, the effect of different GAG species, as well as minor changes in GAG composition on the aggregates formed is yet unknown. If minor changes in GAG composition produce observable changes in liposome aggregate diameter or zeta potential, such a phenomenon may be used to detect potentially dangerous over-sulfated contaminants in heparin. We studied the mechanism of the interactions between heparin and its over-sulfated glycosaminoglycan contaminants with liposomes. Herein, we demonstrate that Mg^{2+} acts to shield the incoming glycosaminoglycans from the negatively-charged phosphate groups of the phospholipids, and that changes in the aggregate diameter and zeta potential are a function of glycosaminoglycan species and concentration, as well as liposome bilayer composition. These observations are supported by TEM studies. We have shown that organizational states of the liposome bilayers are influenced by the presence of GAG and excess Mg^{2+} , resulting in a stabilizing effect which increases the T_m value of DSPC liposomes; the magnitude of this effect is also dependent on GAG species and concentration present. There is an inverse relationship between the percent change of aggregate diameter and percent change of aggregate zeta potential, as a function of GAG concentration in solution. Finally, we demonstrate that the diameter and zeta potential changes of POPC liposome aggregates in the presence of different over-sulfated heparin contaminants at low concentrations allow accurate detection of over-sulfated chondroitin sulfate at concentrations as low as 1 mol%.

INTRODUCTION

Glycosaminoglycans (GAGs) are linear polysaccharides composed of disaccharide units of an amino sugar and uronic acid¹. When incubated with phosphatidylcholine liposomes and divalent cations, GAGs cause the aggregation of liposomes^{2, 3}. The interaction between liposome charge and GAG concentration to cause this effect has been well documented²⁻⁵.

*sanku.mallik@ndsu.edu.

However, studies conducted to date have focused primarily on mechanism of GAG binding, and have limited investigation of how average aggregate diameter and zeta potential are influenced by the species of GAG present in solution. In addition, there is no mention of how average aggregate diameter and zeta potential may co-vary as a function of GAG species and/or concentration, nor is information on how small changes in GAG composition affect these factors presently available. In the current study, we address a number of questions: do liposome aggregates demonstrate differences in their average aggregate diameter and zeta potential as a function of the GAG present in solution? If such changes are observed, how do the original diameter of the liposomes and the concentration of the GAG present influence these changes in aggregate diameter and zeta potential? Finally, if the composition of GAG present in solution varies slightly, can these changes be used to detect these changes? If so, such a phenomenon may prove useful in various industries, particularly the drug industry to detect potentially dangerous over-sulfated contaminants in heparin.

Heparin is a naturally occurring GAG which, when fully sulfated, has three sulfate groups per repeating disaccharide unit, making it the most negatively charged naturally occurring polyelectrolyte in mammalian tissues⁶. Its primary physiological function is highly varied; however its pharmaceutical form (which is typically purified either from porcine intestine or bovine lung) is widely utilized as a drug for the prevention of blood clots in surgery patients⁷.

In 2007 – 2008, several batches of heparin were found to be contaminated with over-sulfated chondroitin sulfate (OSCS), a product prepared by the synthetic oversulfation of chondroitin sulfate⁸, at levels 0.5% by weight to 28% by weight⁹. Over-sulfated chondroitin sulfate has similar but considerably reduced physiological effects as compared to heparin; the anticoagulant effect of oversulfated chondroitin sulfate is approximately 20-25% of that is given by heparin³. In addition, its intravenous administration was associated with numerous allergic reactions, including 149 deaths¹⁰. The adverse effects of oversulfated chondroitin sulfate result from a potent anaphylactic response caused by the activation of the kinin-kallikrein pathway, leading to the release of bradykinin¹¹. Other over-sulfated GAGs have also been shown to modulate this response¹².

To circumvent the onset of above noted side effects, many techniques have been explored/ developed for the detection of over-sulfated GAG contaminants in commercial preparations of heparin. These include ¹H NMR spectroscopy¹³, potentiometric strip tests¹⁴, enzyme immunoassay (ELISA)¹⁵, polyanionic sensors¹⁶, colorimetric assays¹⁷, and activated partial thromboplastin times (aPTT) and prothrombin times (PT) performed with sheep and human plasma¹⁸. While each of these techniques presents advantages, all require specialized equipment, highly-trained personnel, and/or considerable time to obtain results. Approximately one billion doses of heparin are produced each year¹⁹, and therefore a fast, simple, and readily available screen for the presence of over-sulfated contaminants would prove beneficial, both from the safety and economic standpoint. In pursuit of developing easily adaptable and sensitive protocol for detection of oversulfated GAG contaminants in heparin preparations, we investigated the aforementioned tendency of liposomes to aggregate in the presence of GAG and Mg²⁺, varying both liposome diameter and composition, as well as GAG species and concentration. Sensitivity of the changes in aggregate diameter and zeta potential with respect to these parameters were our interest.

EXPERIMENTAL PROCEDURES

Materials, synthesis of over-sulfated GAGs

Chondroitin-6-sulfate, dermatan sulfate, and heparin were sourced from Spectrum Chemical Corp., CalBiochem, and Alfa Aesar, respectively. Each was over-sulfated using the procedures published by Maruyama, et al³ and Nagasawa, et al²⁰.

Preparation of Liposomes for Aggregation

Stock solutions of 1-palmitoyl-2-oleoyl-*sn*-glycero-3-phosphocholine (POPC, commercially available from Avanti Polar Lipids, Alabaster, AL) and 1,2-distearoyl-*sn*-glycero-3-phosphocholine (DSPC, commercially available from Avanti Polar Lipids, Alabaster, AL) were prepared in chloroform at a concentration of 2 mg/mL. Stock solution of 1,2-dipalmitoyl-*sn*-glycero-3-phosphoethanolamine-N-(lissamine rhodamine B sulfonyl) (ammonium salt) (rhodamine lipid, commercially available from Avanti Polar Lipids, Alabaster, AL) was prepared in chloroform at a concentration of 0.01 mg/mL. Stock solution of pyranine lipid was prepared in chloroform at a concentration of 0.01 mg/mL. Lipid mixtures containing POPC were obtained by combining 2.4 mL POPC stock solution, and either 8.0 mL rhodamine lipid stock solution or 8.4 mL pyranine lipid stock solution. Mixtures containing DSPC were prepared by combining 2 mL DSPC stock solution and 6.5 mL rhodamine lipid stock solution.

The resulting mixtures had molar ratios of 99:1 POPC (or DSPC):rhodamine lipid/pyranine lipid, respectively. The mixture was subjected to rotary evaporation at 50°C for 15 minutes, forming a thin film adhering to the sides of the flask. This thin film was then dried overnight under high vacuum to ensure complete removal of solvent. Lipid films containing POPC as the main lipid were then hydrated with 4.0 mL of 25 mM HEPES buffer at pH 8 by rapid rotation in a 50°C water bath for 1hr. Lipid films containing DSPC as the main lipid were hydrated with 4.0 mL of 25 mM HEPES buffer at pH 8 by rapid rotation in a 70°C water bath for 1hr. The procedure now varies for production of 50 nm, 200 nm, and 500 nm liposomes:

- For 50 nm diameter liposomes (POPC liposomes only): the hydrated solution was probe sonicated at 70°C for 45 minutes, followed by extrusion at 70 °C (15 times) through polycarbonate membrane filters (100 nm pore size). The average diameter of the prepared liposomes (by DLS) was approximately 55 nm + 25 nm.
- For 200 nm diameter liposomes (POPC and DSPC liposomes): the hydrated solution was immediately extruded at 70 °C (15 times) through polycarbonate membrane filters (100 nm pore size). Average measured diameters (by DLS) were approximately 185 + 8 nm and 250 + 90 nm for POPC and DSPC liposomes, respectively.
- For 550 nm diameter liposomes (POPC liposomes only): Following hydration, the resulting large vesicles were found to have an average diameter of 550 + 70 nm (by DLS). These liposomes were used as such.

The final volume of each respective liposome solution was then measured using the extrusion syringes, and the total lipid per unit volume calculated from this volume. All liposome solutions were diluted to 1.4 mM total lipid before use. We have tested the same batches of diluted liposomes multiple times over up to two months. The size of the liposomes did not change during the two month time period, and the aggregation and zeta potential during this time period have been extremely consistent.

Mechanistic Studies--Influence of GAG species and Mg²⁺ on diameter and zeta potential of aggregates

DSPC or POPC liposomes (200 nm diameter only) were incubated for 15 minutes at room temperature in the presence and absence of Mg²⁺ (33.4 mM final concentration), as well as the presence and absence of heparin. Mixtures were produced according to Table 1 below.

Each mixture was allowed to incubate at room temperature for 15 minutes before reading. One hundred μL of this aggregated solution was mixed with 900 μL HEPES buffer at pH 8 in a disposable polystyrene cuvette, and read on a Malvern Zetasizer Nano ZS90 with the following settings: 5 measurements, each an average of 10 reads, each read 10 sec; 90° read angle; 60 second pre-equilibration; Auto Attenuation off, manual attenuation set to 7. For the corresponding zeta potential measurements, liposomes were aggregated in the same way as above. Zeta potential was read on a Malvern Zetasizer Nano ZS90 with the following settings: 5 measurements, each an average of 10 reads, each read 10 seconds; 60 second pre-equilibration; automatic attenuation on; automatic voltage selection on.

Mechanistic Studies--Influence of GAG species and concentration on the saturation of aggregate diameter and zeta potential

For tests with individual GAGs, POPC and DSPC liposomes were aggregated in the presence of eight different concentrations of each GAG (heparin, over-sulfated chondroitin sulfate, over-sulfated dermatan sulfate, or over-sulfated heparin) in preparation for DLS, according to Table 2 below.

Measurement of aggregate diameter and zeta potential proceeded in the same way as stated above. Three measurements were collected for each GAG concentration for both average diameter and zeta potential, each an average of 10 reads, each read 10 seconds. Equipment settings remained the same.

TEM Imaging

To aggregate liposomes, 50 μL of liposomes (200 nm diameter) at 1.4 mM, were incubated with 60 μL of GAG at 1 μM (approximately 20% v/v, 170 nM final concentration) and 6 μL of MgSO₄ at 2 M in 240 μL HEPES buffer at pH 8 for 15 minutes at room temperature. For liposome only control, 60 μL GAG was substituted with 60 μL additional HEPES buffer. Copper TEM grids (300-mesh, formvar-carbon coated, Electron Microscopy Sciences, Hatfield, Pennsylvania, USA) were prepared by applying a drop of 0.01% poly-L-lysine, allowing it to stand for 30 seconds, wicking off the liquid with torn filter paper, and allowing the grids to air dry. A drop of the aggregated liposome suspension was placed on a prepared grid for 30 seconds and wicked off; grids were allowed to air dry again. Phosphotungstic acid 1%, pH adjusted to 7-8, was dropped onto the grid containing the liposome sample, allowed to stand for 1.5 min, and wicked off. After the grids were dry, images were obtained using a JEOL JEM-2100 LaB₆ transmission electron microscope (JEOL USA, Peabody, Massachusetts) running at 200 keV.

Differential Scanning Calorimetry

DSPC liposomes were incubated with 1 μM and 250 μM GAG for 15 minutes at room temperature, before being degassed for 15 minutes and loaded into a Nano DSC (TA instruments New Castle, DE) without further dilution. A sample of DSPC liposomes incubated with only Mg²⁺ was used as the control. The DSC reference cell was filled with HEPES buffer at 25 mM, pH 8, containing 33.4 mM MgSO₄, the same as that of the samples. Machine was pressurized to three atmospheres, and scans were conducted from 25 °C to 75 °C, and rate of temperature change was 2 °C/minute. Heat required during

transition was calculated using NanoAnalyze software provided by the instrument vendor, using the sigmoidal baseline function to produce the pre- and post-transition baseline.

Mechanistic studies—combined influence of liposome diameter and GAG concentration on diameter and zeta potential changes

POPC liposomes of diameters 50, 200, and 550 nm diameter liposomes were each incubated with heparin, OSH, OSCS, and OSD (individually) at concentrations of 50, 170, and 500 nM. Measurement of aggregate diameter and zeta potential were measured in the same way as stated above. Five measurements were collected for each GAG concentration for both diameter and zeta potential, each an average of 10 reads, each read 10 seconds. Equipment settings remained the same. Following collection of data, each over-sulfated contaminant was compared to the corresponding measurement of heparin by calculating the percent change from heparin, using the following formula:

$$\left(\frac{\text{size of contaminant aggregate} - \text{size of heparin aggregate}}{\text{size of heparin aggregate}} \right) \times 100$$

The same formula was applied to calculate zeta potential percent change.

Heparin contamination studies

For contaminated heparin studies, final concentrations of 170 nM and 500 nM total GAG were used with 200 nm and 500 nm diameter liposomes, respectively. Solutions of heparin with an over-sulfated contaminant were prepared according to Tables 3 and 4 below.

Measurement of aggregate diameter and zeta potential proceeded in the same way as stated above. Five measurements were collected for each GAG concentration for both diameter and zeta potential, each an average of 10 reads, each read 10 seconds. Equipment settings remain the same.

Statistical Analysis

Analysis of variance and Dunnett's post-tests were run using Minitab software, version 16.1.1.

RESULTS AND DISCUSSION

In our previous work, we have demonstrated that phosphocholine liposomes having either the pyranine lipid or the lissamine-rhodamine lipid present in the bilayer at 1 mol% were able to distinguish between different GAG species in solution²¹. In these studies, we have found the optimal liposomes for GAG discrimination contain the pyranine or the rhodamine lipid (Figure 1 shows structures of these lipids); however preliminary studies demonstrated that liposomes containing the pyranine head group tend to aggregate in the presence of excess of divalent cations (i.e., in the absence of GAG; data not shown). Based on these prior results, we prepared 1-palmitoyl-2-oleoyl-*sn*-glycero-3-phosphocholine (POPC) liposomes incorporating 1 mol% of 1,2-dipalmitoyl-*sn*-glycero-3-phosphoethanolamine-N-(lissamine rhodamine B sulfonyl; rhodamine lipid), as well as 1,2-distearoyl-*sn*-glycero-3-phosphocholine (DSPC) liposomes incorporating 1 mol% rhodamine lipid for use in these studies. We employed transmission electron microscopy (TEM) and dynamic light scattering (DLS) to evaluate the relative diameter differences between aggregates produced by different GAGs. Changes in diameter and zeta potential in the presence of different GAGs were also evaluated. We used DLS and zeta potential changes to determine if there are any variations upon contamination of heparin with over-sulfated GAGs. Inclusion of the

fluorophore in the liposomal bilayer was originally intended for study of fluctuations in fluorescence emission intensity as a function of the aggregation phenomenon. However, due to non-uniformity of the liposomal solution upon aggregation, fluorescence studies produced very variable results, and were thus removed from this study.

Preparation of liposomes

We have previously shown that 100 nm diameter liposomes composed of 99 mol% POPC and 1 mol% fluorophore-conjugated lipid (either pyranine, rhodamine, or dansyl) are able to discriminate between various GAGs²¹. Although these liposomes undergo modulations in fluorescence intensity in the presence of GAGs only, we wish to utilize the tendency of these liposomes to undergo rapid changes in the aggregate diameter and zeta potential in the presence of GAG and divalent cations to develop a rapid screen for these contaminants. To achieve this, we have chosen Mg^{2+} as a flocculating agent²², and have produced POPC liposomes of three diameters (50, 200, and 550 nm) and aggregated each of these in the presence of three concentrations (50, 170, and 500 nM) of each GAG of interest: heparin, over-sulfated heparin (OSH), over-sulfated chondroitin sulfate (OSCS), and over-sulfated dermatan sulfate (OSD). We demonstrate that high concentrations of Mg^{2+} aggregate liposomes in the presence of GAG, but not in the absence of GAG (as shown in Tables 5 and 6).

Mechanistic studies: liposomes selectively aggregate upon binding of different GAG species when Mg^{2+} is present, and liposome-GAG interactions influence the zeta potentials and diameters of overall assembly

Kim and Nishida had proposed that the divalent cation (Mg^{2+} in our case) form bridges between the negative phosphate groups of the phospholipid head groups⁵. This interaction shields the incoming GAGs from the negative charges on liposome surface, allowing them to bind to the positively charged choline⁵. To study this effect, we used both DSPC-rhodamine liposomes and POPC-rhodamine liposomes (200 nm diameter) in the presence of Mg^{2+} only, in the presence of each GAG only (no Mg^{2+}), and finally in the presence of both GAG and Mg^{2+} (GAG concentration was held constant at 170 nM). Both diameters and zeta potentials of the resulting aggregates were measured. Results of these studies are as shown in Tables 5 and 6.

As the zeta potentials of both POPC and DSPC-containing liposomes does not appear to change significantly without the presence of Mg^{2+} , we conclude that the GAGs alone do not bind to the surface of liposomes, as has been previously reported⁴. However in contrast to previous studies⁴, we find that excess Mg^{2+} does result in liposomal charge inversion²³, changing the zeta potential of the liposomes. It is likely that previous studies did not use divalent cations in sufficiently large excess to observe this effect. Consistent with previous findings, we note a significant change in the zeta potential upon the addition of both Mg^{2+} and GAG in the presence of DSPC liposomes; however this effect is negligible for POPC liposomes. Interesting to note is the drop in zeta potential of the DSPC aggregates to -16 mV in the presence of OSCS, 4 mV below that of the original liposomes. This effect likely results from overcharging of the liposome surface, due to excess charge from the OSCS²³. Both liposomes experience significant changes in aggregate diameter in the presence of GAG and Mg^{2+} , and these diameter changes appear to be dependent on the species of GAG present, particularly for POPC liposomes. Literature reports on the measurement of zeta potential in the presence of liposomes aggregated by glycosaminoglycans have found that the aggregation does not interfere with the measurement of zeta potential².

Mechanistic studies: Diameter and zeta potential of liposome aggregates reach saturation upon addition of sufficient concentrations of GAG

To determine how the aggregate hydrodynamic diameters and zeta potentials of both DSPC and POPC containing liposomes changed with increasing concentrations of each GAG, and to determine if there were any differences between GAGs at these concentrations, DSPC and POPC liposomes were incubated with heparin, over-sulfated chondroitin sulfate, over-sulfated dermatan sulfate, and over-sulfated heparin at eight concentrations (100 nM, 500 nM, 1 μ M, 10 μ M, 50 μ M, 100 μ M, 250 μ M, and 500 μ M). Results are summarized in Figure 2 below; each data point is the average of three collected aggregate diameter or zeta potential measurements. We note that some of the diameter measurements are outside the range which the Zetasizer Nano may accurately measure (5×10^3 nm diameter), however the purpose of these experiments was to investigate whether each species of GAG caused the eventual saturation of both aggregate diameters and zeta potentials, and if so above what concentration does this saturation take place. Measurements are of interest in terms of general trend only.

Notable are the progression of aggregate diameters from small to quite large and then to small again for both DSPC and POPC containing liposomes, as concentration increases. This is consistent with theoretical analysis of McClements²⁴ and Guzey²⁵, according to which below a specific critical concentration of charged polymers (e.g., GAGs), the surface of the colloid particles (liposomes) will be incompletely covered by the polymer, resulting in an imbalance between attractive and repulsive forces acting on the colloidal particles. Below this critical concentration, these imbalances will allow sections of liposome surface coated with GAG to attract sections of neighboring liposomes which have not been so coated, resulting in aggregate formation. Above this critical concentration however, the surfaces of the colloidal particles will become saturated as the charged polymer forms a continuous coat on the surface, and allows the repulsive forces between the colloid particles in solution to become re-balanced, preventing significant aggregation. McClements²⁴ also notes that at concentrations much higher than the critical concentration may cause “depletion flocculation” due to excesses of polymer electrolyte in solution, which may be sufficient to overcome the repulsive forces between colloid particles. This depletion flocculation may be one explanation for the sudden increase in diameter of the POPC liposomes in presence of 500 μ M over-sulfated heparin.

For the DSPC containing liposomes, as the aggregate diameter becomes saturated, the zeta potential becomes likewise saturated (at high GAG concentration), and does not change appreciably at higher concentrations. For the POPC containing liposomes however, there is a tendency for the zeta potential to reach a minimum, and then return to smaller absolute values at higher concentrations. This difference is clearly due to the difference in composition of the fatty acid tails of the liposomal lipids. In the case of DSPC, both tails are constituted of saturated (stearic acid) and thus they will pack more efficiently (*vis a vis* the palmitoyl and oleyl tails of POPC) within the lipid phase. These differences will impart greater rigidity to the head groups of the DSPC liposomes, and thus will allow homogeneous distribution of GAG induced aggregates of the liposomes. The above feature is unlikely to prevail in the case of POPC liposomes. It is worth noting that other studies involving changes in the liposome's zeta potential upon addition of GAGs and divalent cations were focused on lipid bilayers, harboring saturated lipids (DMPC, DLPC, and egg lecithin)^{2, 4}, and these studies produced zeta potential results similar to our DSPC liposomes. However, irrespective of the underlying physical forces responsible for our observed experimental data of Fig.2, it is evident that POPC and DSPC formulated liposomes elicit marked differences in their aggregational states and zeta potentials as a function of different types of GAGs. Whether or not such features are intimately involved in discriminatory changes in the liposome's resident fluorescence probes²¹ as a function of different types of GAGs are

currently being investigated in our laboratory, and we will report these findings subsequently.

TEM images demonstrate differential aggregation of liposomes in the presence of different GAG species

The diameters of the POPC liposomes and DSPC liposomes in the presence of Mg^{2+} only were compared with those in the presence of heparin, over-sulfated chondroitin sulfate, over-sulfated dermatan sulfate, and over-sulfated heparin. Figure 3 presents the TEM images of the POPC liposomes in the presence of Mg^{2+} alone (panel **A**) and in the presence of Mg^{2+} and different GAG species. Figure 4 presents the corresponding TEM images involving DSPC liposomes. In each figure, panels **A-E** are images of liposomes magnified 5,000 times, and panel **F** is an image of one OSCS aggregate magnified 25,000 to show detail of the stacked liposomes. The TEM images of Figures 3 and 4 clearly reveal that the liposomes are aggregated in the presence of Mg^{2+} and different GAG species, and such aggregates are asymmetrical and polydisperse. However, notable in these TEM images is the presence of considerably larger aggregates in the presence of over-sulfated GAGs as compared to those observed in the presence of heparin. Also notable is the apparent size in these images; it is evident that the liposomes and aggregates have collapsed during the preparation of the samples. It is therefore necessary to consider these sizes as relative; aggregate images should only be compared with images of the liposomes in the presence of Mg^{2+} only.

Differential scanning calorimetry demonstrates intrinsic and differential stability of liposomes upon binding of GAGs to liposomes

Having established that the liposomes are aggregated in the presence of both Mg^{2+} and different GAG species, it was of interest to investigate whether the above “effectors” modulated the intrinsic stability of liposomes. To probe this, we performed DSC studies for melting of DSPC liposomes in the presence of Mg^{2+} and two concentrations (i.e., 1 μ M and at 250 μ M) of each different GAG species. The DSC endotherms reveal that the presence of Mg^{2+} and GAGs influence both the melting temperature (T_m value) of the liposomes as well as the area under the peaks (measure of the enthalpic changes between native and denatured/melted forms of the liposomes; see Figure 5). The observed shifting of the 250 μ M trace to a lower relative heat rate reflects the increase of dissolved solutes over the control²⁶, and the widening and flattening of the DSC trace with increasing GAG concentration, accompanied by a rightward shift in T_m , indicates that structural changes are taking place within the bilayers of the liposomes (increased T_m), and that these changes are dispersed somewhat unevenly within the “population” of the liposomes (widening and flattening of the T_m peak)²⁶. To our further interest, we observed that the second DSC scan (performed after cooling the heated sample after the first scan) yielded essentially identical T_m values in the presence of different GAG species, albeit the enthalpic changes were slightly decreased (data not shown). This suggests that there is a marked reversibility in the organizational states of the liposomes, and such feature is intrinsic to the nature of the GAG species. Table 7 summarizes the T_m values and enthalpic changes under our selected experimental conditions. A perusal of the data of Table 6 reveals that among different GAGs used herein, heparin and oversulfated heparin exhibit the least and most stabilizing influence on the liposomes as evident by their corresponding enthalpic changes.

We conclude from these studies that binding of GAGs and Mg^{2+} to the liposomal bilayer causes the liposomal assembly to become more stable, and thus requires more heat energy (enthalpic changes) to bring it to the fully disorganized (melted) states with concomitant increase in the transition temperature. We believe the above feature is due to the intercalation of the GAGs between the individual phosphocholine molecules, thus forcing

the exclusion of intervening water molecules and thus allowing the liposomal lipids to pack more efficiently in their native states.

Mechanistic studies: there is an inverse relationship between the percent change of aggregate diameter and the percent change of aggregate zeta potential as the concentration of GAG increases, independent of liposome diameter

For studies comparing the relative contribution of liposome diameter and GAG concentration to the overall average diameter and zeta potential changes of the resulting aggregates, only POPC liposomes were used. This is due to the high variability of the DSPC liposomes' diameters, which is clear from results shown in Table 6 (the standard deviation for the diameter of these liposomes alone as measure by DLS is 36% of their diameter). Additionally, DLS shows the presence of both very large (>1000 nm) and very small (<50 nm) particles in the DSPC liposome solution. Due to this difficulty in controlling the liposome diameter, DSPC liposomes have been excluded from this, as well as the contamination studies.

As one considers the percent change of each over-sulfated contaminant relative to heparin at each concentration, while holding the diameter of the liposomes constant, an interesting pattern emerges: there appears to be an inverse relationship between the percent change in aggregate diameters, and the percent change in aggregate zeta potential (i.e.—as the percent change in diameter goes down with increasing GAG concentration, the percent change in zeta potential becomes greater with increasing GAG concentration). These results are summarized in Figure 6.

Notable from this figure is that at 50 nM concentration (represented by a black trace with black squares), OSCS always produces the greatest change in aggregate diameter, regardless of the liposomes' starting diameter. At 170 nM GAG, OSD causes the greatest changes in aggregate diameter, and at 500 nM GAG results depend on the starting liposome diameter. Reasons for this are unclear, and will require further investigation. However it is obvious from these results that as GAG concentration increases, overall percent change decreases. Results for percent change in aggregate zeta potential are also very consistent for liposomes of all diameters tested: as GAG concentration increases, the magnitude of percent change in aggregate zeta potential also increases. We hypothesize the mechanism for this may be due to differences in the percent overall coverage of the liposome surface by the GAG. When the concentration of GAG in solution is relatively low relative to the total lipid concentration in solution (~200 nM), the liposomal surface is covered with GAG to a lesser extent, resulting in greater imbalance between the attractive and repulsive colloidal forces. As such, the number of liposomes which form aggregates will be dependent on the charge density of the GAG present on the liposome surface, as well as the surface area between oppositely charged sections of each bilayer (a function both of liposome diameters and the percent of surface area covered). However, as the concentration of GAG in solution increases, the surface of each liposome bilayer will be covered to a greater extent, which will not only begin to re-balance the repulsive forces between them in solution, but it will also reduce the amount of available surface area for aggregation between liposomes. This will reduce the percent change in the aggregate diameter (as fewer liposomes will be able to aggregate together), as well as increasing the change observed in the zeta potentials (as a function of the amount and charge density of the GAG bound). Studies to confirm this mechanism are currently being undertaken.

Contamination studies demonstrate that changes in diameter and zeta potential of POPC liposomes can distinguish small changes in GAG composition

The insights gained from the previous studies were employed to probe whether the presence of low concentrations of over-sulfated contaminants in a heparin sample could be detected using DLS and zeta potential measurements of liposomal aggregates. We chose to incubate 200 nm diameter liposomes with 170 nM contaminated heparin (produced the greatest percent changes in diameter), and 500 nm diameter liposomes with 500 nM contaminated heparin (produced the greatest percent changes in zeta potential). Heparin samples in 2008 were found by Beyer, et al, to be contaminated in the range of 0.5% to 28% by weight⁹. As such, for both of these liposome/GAG concentration combinations, eight contamination levels were prepared: 0.5, 1.0, 2.5, 5, 10, 15, 20, and 30 mol% contaminations with each over-sulfated contaminant. Each combination was measured for changes in aggregate diameter and zeta potential by DLS.

Analysis of variance ($\alpha = 0.05$) was conducted for each of these sets of data (see statistical results in Supporting Information). Included in this analysis is a comparison of means for each contamination level against heparin alone using Dunnett's method for pairwise comparisons²⁷. This method allows us to compare each contamination level to the control (heparin only) while controlling the family-wise error of all comparisons together to 0.05. Results for both 200 nm and 500 nm diameter liposomes indicate that OSH could not be consistently detected, and thus will be eliminated from further discussion.

Results for OSCS and OSD are far more promising. Analysis of variance indicates that for the 200 nm liposomes, changes in average aggregate diameter could detect contamination by OSCS at concentrations from 5 mol% to 30 mol%, and OSD contamination from concentrations of 10 mol% to 30 mol%. Changes in aggregate zeta potential could not consistently detect contamination. Results for the 500 nm diameter liposomes indicate detection of OSCS contamination at concentrations from 1 mol% through 30 mol% by changes in zeta potential, and from 2.5 mol% to 30 mol% by changes in aggregate diameter. OSD could be detected by this method from 10 mol% to 30 mol% by changes in zeta potential, and from 0.5 mol% to 30 mol% by changes in aggregate diameter. (For detailed statistical results please see Supporting Information). If we consider percent heparin contamination by weight, the lowest contamination level we can detect using these methods is approximately 1.6% by weight of OSD, and 2.2% by weight of OSCS, making it an attractive screening tool for heparin intended for clinical use. These calculations are based on the estimated molecular weights of heparin, over-sulfated chondroitin sulfate, and over-sulfated dermatan sulfate, summarized in Table 8 below.

It must be stated that despite the relative consistency and significance of the DLS diameter measurements, the presence of fluorescence, high polydispersity, and large precipitating particles in the sample lead us to favor the use of zeta potential for measurements of over-sulfated heparin contaminants, as these measurements are unaffected by any of the aforementioned concerns.

A comparison of current methods used to detect heparin quality reported in 2011 by Alban, et al., has been very revealing. The authors reported that while NMR and other spectroscopic methods are useable, other heparin mimetic may cause deviating results, and thus accurate detection of OSCS in heparin will be in large part dependent on the skill of the individual running the tests, and only currently known heparin contaminants may be recognized¹⁸. Additionally, the PT and aPTT, while they are able to detect overall heparin quality, cannot actually detect contamination, and have an LOD of 3%¹⁸. Further, it must be recognized that no reported adverse effects were observed from enoxaparin contaminated with up to 7% OSCS¹⁵. Based on this, the analysis by Alban and Beyer of original contaminated

samples^{9, 18}, and the above statistical analysis of our data, we believe that zeta potential measurements combined with DLS diameter measurements of POPC based liposomes incubated with heparin samples at 170/500 nM and excess Mg²⁺ may be a rapid and economical initial screen for contamination in these samples.

CONCLUSIONS

We have demonstrated that liposomes containing 1 mol% lissamine-rhodamine lipid form aggregates of varying diameters and zeta potentials depending on the species and concentration of GAG present. This has been verified by TEM studies. We have shown that organizational states of the liposome bilayers are influenced by the presence of GAG and excess Mg²⁺, resulting in a stabilizing effect, and the magnitude of this effect is also dependent on GAG species and concentration present. Additionally, there is an inverse relationship between the percent change of aggregate diameter and percent change of aggregate zeta potential, as a function of GAG concentration in solution. Finally, the presence of small concentrations of over-sulfated contaminants in heparin samples cause statistically significant variations in the average aggregate diameter and zeta potential POPC liposomes. Significant variations of POPC liposome aggregate zeta potentials enables detection of over-sulfated chondroitin sulfate and over-sulfated dermatan sulfate at 1 mol% and 0.5 mol % (2.2% w/w and 1.6% w/w, respectively). Based on the work of Bayer, the use of this method would have been able to detect the contaminants in the majority of the original heparin samples which caused allergic reactions and deaths of patients in 2007 and 2008⁹. These results offer insight into the potential of these interactions for a rapid and economical screen for the presence of over-sulfated contaminants in heparin or other drugs.

Supplementary Material

Refer to Web version on PubMed Central for supplementary material.

Acknowledgments

This research was supported by NIH grants 1R01 CA CA113746, 1R01 CA 132034 to SM and DKS and NSF grant DMR 1005011 to SM. The ITC and the DSC instruments were purchased through the NSF ARRA award CBET-0959422.

REFERENCES

1. Zhang, F.; Zhang, Z.; Linhardt, RJ. *The Handbook of Glycomics*. Elsevier; London, UK: 2009.
2. Krumbiegel M, Arnold K. Microelectrophoresis studies of the binding of glycosaminoglycans to phosphatidylcholine liposomes. *Chemistry and Physics of Lipids*. 1990; 54:1–7. [PubMed: 1694471]
3. Satoh A, Toida T, Yoshida K, Kojima K, Matsumoto I. New role of glycosaminoglycans on the plasma membrane proposed by their interaction with phosphatidylcholine. *FEBS Letters*. 2000; 477:249–252. [PubMed: 10908729]
4. Zschornig O, Richter W, Paasche G, Arnold K. Cation-mediated interaction of dextran sulfate with phospholipid vesicles: binding, vesicle surface polarity, leakage and fusion. *Colloid Polymer Science*. 2000; 278:637–646.
5. Kim YC, Nishida T. Nature of interaction of dextran sulfate with lecithin dispersions and lysolecithin micelles. *J Biol Chem*. 1977; 252(4):1243–9. [PubMed: 838715]
6. Voet, D.; Voet, J. *Biochemistry*. 3rd ed. John Wiley & Sons, Inc.; Hoboken, NJ: 2004.
7. Linhardt RJ, Claude S. Hudson award address in carbohydrate chemistry. Heparin: Structure and Activity. *Journal of Medicinal Chemistry*. 2003; 46:2551–2564. [PubMed: 12801218]

8. Maruyama T, Toida T, Imanari T, Yu G, Linhardt R. Conformational changes and anticoagulant activity of chondroitin sulfate following its O-sulfonation. *Carbohydrate Research*. 1998; 306:35–43. [PubMed: 9691438]
9. Beyer T, Matz M, Brinz D, Radler O, Wolf B, Norwig J, Baumann K, Alban S, Holzgrabe U. Composition of OSCS-contaminated heparin occurring in 2008 in batches on the German market. *Eur J Pharm Sci*. 2010; 40(4):297–304. [PubMed: 20399266]
10. Pan J, Qian Y, Zhou X, Pazandak A, Frazier SB, Weiser P, Lu H, Zhang L. Oversulfated chondroitin sulfate is not the sole contaminant in heparin. *Nature Biotechnology*. 2010; 28(3):203–207.
11. Li B, Suwan J, Martin JG, Zhang F, Zhang Z, Hoppensteadt D, Clark M, Fareed J, Linhardt RJ. Oversulfated chondroitin sulfate interactions with heparin-binding proteins: New insights into adverse reactions from contaminated heparins. *Biochemical Pharmacology*. 2009; 78:292–300. [PubMed: 19389385]
12. Pan J, Qian Y, Zhou X, Lu H, Ramacciotti E, Zhang L. Chemically oversulfated glycosaminoglycans are potent modulators of contact system activation and different cell signaling pathways. *Journal of Biological Chemistry*. 2010; 285(30):22966–22974. [PubMed: 20418371]
13. Zhang Z, Li B, Suwan J, Zhang F, Z W, Liu H, Mulloy B, Linhardt R. Analysis of pharmaceutical heparins and potential contaminants using ¹H-NMR and PAGE. *Journal of Pharmaceutical Sciences*. 2009; 98:4017–4026. [PubMed: 19642166]
14. Kang Y, Gwon K, Shin JH, Nam H, Meyerhoff M, Cha G. Highly sensitive potentiometric strip test for detecting high charge density impurities in heparin. *Analytical Chemistry*. 2011; 83:3957–3962. [PubMed: 21500820]
15. Bairstow S, McKee J, Nordhaus M, Johnson R. Identification of a simple and sensitive microplate method for the detection of oversulfated chondroitin sulfate in heparin products. *Analytical Chemistry*. 2009; 288:317–321.
16. Wang L, Buchanan S, Meyerhoff M. Detection of high-charge density polyanion contaminants in biomedical heparin preparations using potentiometric polyanion sensors. *Analytical Chemistry*. 2008; 80:9845–9847. [PubMed: 19007240]
17. Sommers C, Mans D, Mecker L, Keire D. Sensitive detection of oversulfated chondroitin sulfate in heparin sodium or crude heparin with a colorimetric micro plate based assay. *Analytical Chemistry*. 2011; 83:3422–3420. [PubMed: 21449571]
18. Alban S, Luhn S, Schiemann S, Beyer T, Norwig J, Schilling C, Radler O, Wolf B, Matz M, Baumann K, Holzgrabe U. Comparison of established and novel purity tests for the quality control of heparin by means of a set of 177 heparin samples. *Anal Bioanal Chem*. 2011; 399(2):605–20. [PubMed: 20824424]
19. Bertozzi, CR.; Freeze, HH.; Varki, A.; Esko, JD. *Glycans in biotechnology and the pharmaceutical industry*. Cold Spring Harbor Laboratory Press; Cold Spring Harbor, NY: 2009.
20. Nagasawa K, Uchiyama H, Wajima N. Chemical sulfation of preparations of chondroitin 4- and 6-sulfate, and dermatan sulfate. Preparation of chondroitin sulfate E-like materials from chondroitin-4-sulfate. *Carbohydrate Research*. 1986; 158:183–190.
21. Nyren-Erickson EK, Haldar MK, Gu Y, Qian SY, Friesner DL, Mallik S. Fluorescent liposomes for differential interactions with glycosaminoglycans. *Analytical Chemistry*. 2011; 83(15):5989–5995. [PubMed: 21675793]
22. Semerjian LA, G. M. 7High-pH–magnesium coagulation–flocculation in wastewater treatment. *Advances in Environmental Research*. 2003; 7(2):389–403.
23. Hsiao PY. Overcharging, charge inversion, and reentrant condensation: using highly charged polyelectrolytes in tetravalent salt solutions as an example of study. *J Phys Chem B*. 2008; 112(25):7347–50. [PubMed: 18517240]
24. McClements DJ. Theoretical analysis of factors affecting the formation and stability of multilayered colloidal dispersions. *Langmuir*. 2005; 21:9777–9785. [PubMed: 16207066]
25. Guzey D, McClements DJ. Formation, stability and properties of multilayer emulsions for application in the food industry. *Adv Colloid Interface Sci*. 2006; 128-130:227–48. [PubMed: 17223060]

26. Gabbott, P. Principles and applications of thermal analysis. Blackwell Pub.; Oxford ; Ames, Iowa: 2008. p. xviii. 464
27. Mendenhall, W.; Sincich, T. A second course in statistics : regression analysis. 7th ed. Pearson Education; Boston: 2012.

\$watermark-text

\$watermark-text

\$watermark-text

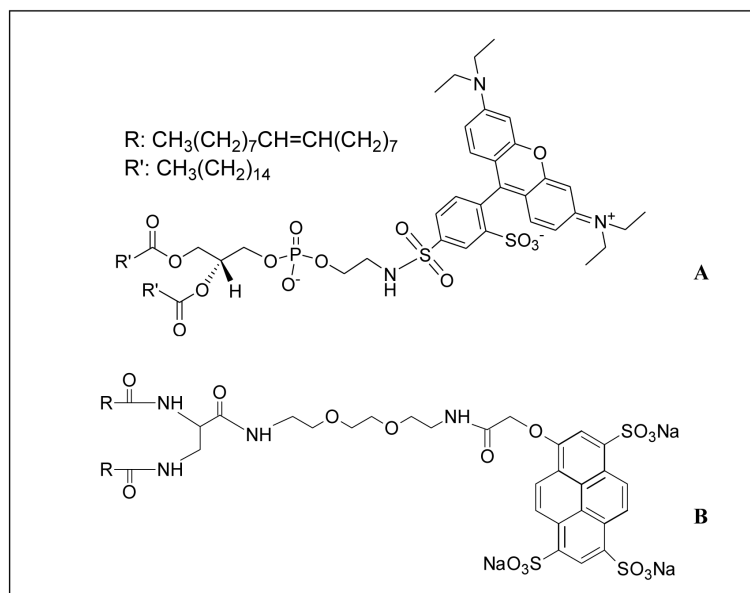


Figure 1.
Structures of rhodamine (A) and pyranine (B) lipids.

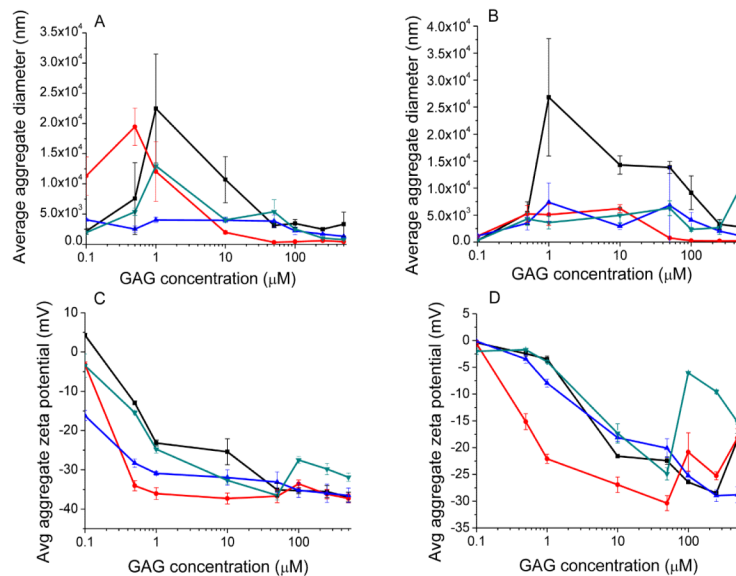


Figure 2. Average aggregate diameters of DSPC liposome aggregates (**A**) and POPC liposomes (**B**); and average zeta potentials of DSPC liposome aggregates (**C**) and POPC liposomes (**D**) in the presence of increasing concentrations of heparin (black squares), over-sulfated chondroitin sulfate (blue triangles), over-sulfated dermatan sulfate (red circles), and over-sulfated heparin (green upside-down triangles).

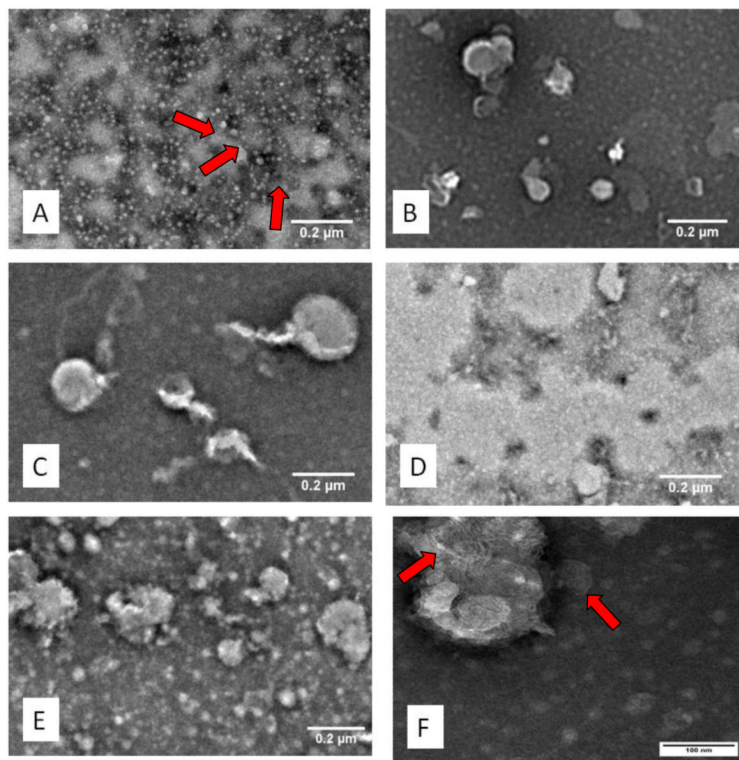


Figure 3.

TEM images of POPC liposomes with Mg^{2+} only (**A**): red arrows denote individual liposomes), and aggregated in the presence of heparin (**B**), over-sulfated chondroitin sulfate (**C**), over-sulfated dermatan sulfate (**D**), and over-sulfated heparin (**E**) magnified 5,000x. Notable is the increase in average size of the aggregates of over-sulfated GAGs over heparin, as well as the polydispersity of these aggregates. Shown also is an image of liposomes aggregated with over-sulfated chondroitin sulfate magnified 25,000x (**F**). Clearly shown are the clustered bilayers in one section of the aggregate, denoted by the red arrows.

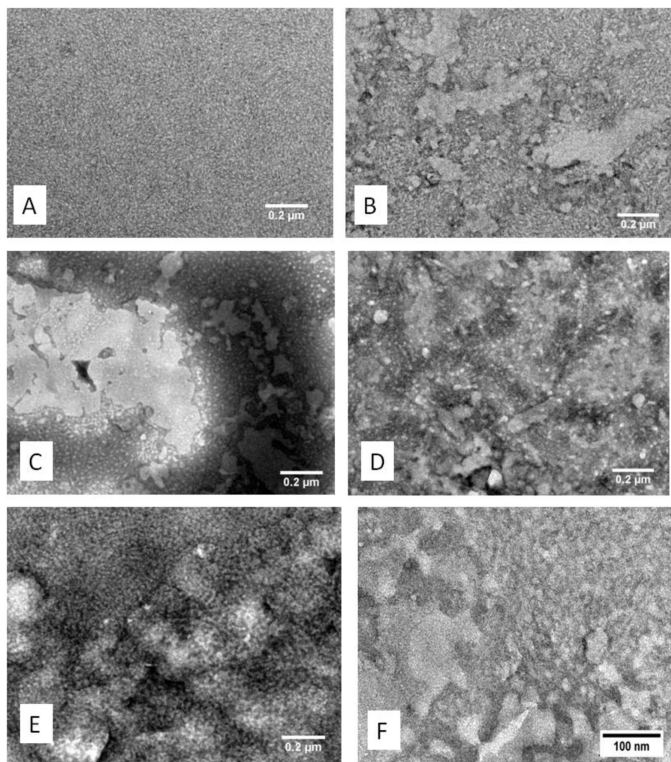


Figure 4. TEM images of DSPC liposomes with Mg^{2+} only (**A**), and aggregated in the presence of heparin (**B**), over-sulfated chondroitin sulfate (**C**), over-sulfated dermatan sulfate (**D**), and over-sulfated heparin (**E**) magnified 5,000x. Notable is the polydispersity of these aggregates. Shown also is an image of liposomes aggregated with over-sulfated chondroitin sulfate magnified 25,000x (**F**). Visible are the closely associated liposomes within a single aggregate.

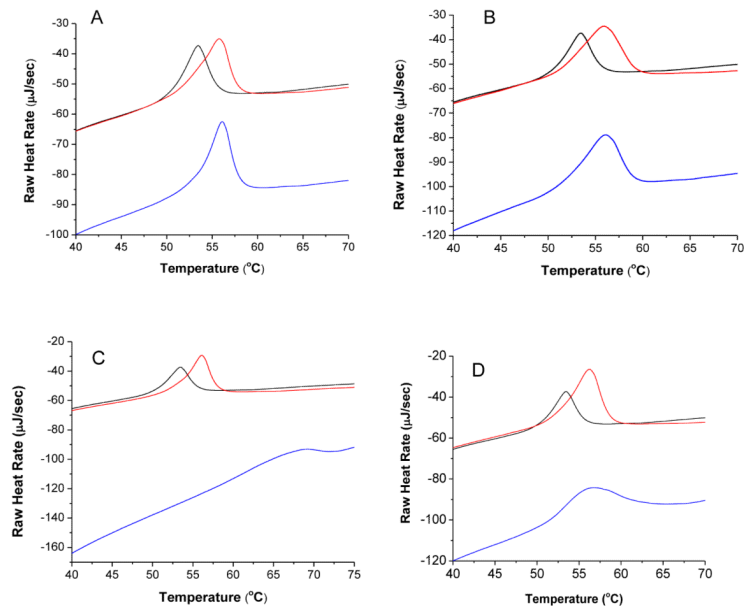


Figure 5. DSC traces of DSPC liposomes with heparin (**A**), over-sulfated chondroitin sulfate (**B**), over-sulfated dermatan sulfate (**C**), and over-sulfated heparin (**D**): liposomes only (black trace), GAG at 1 μM (red trace), GAG at 250 μM (blue trace).

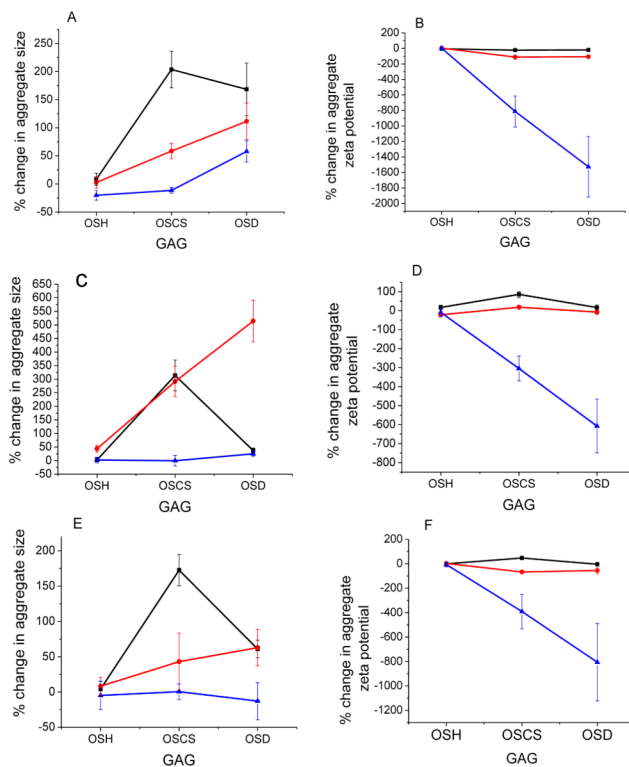


Figure 6. Percent changes for 50 nm diameter liposomes (A, B), 200 nm liposomes (C, D), and 500 nm liposomes (E, F). Shown are percent changes in aggregate diameter (A, C, E) and percent changes in aggregate zeta potential (B, D, F). Concentrations used for this study are 50 nM (black squares), 170 nM (red circles), and 500 nM (blue triangles).

Table 1Preparation of liposomes for diameter and zeta potential mechanism tests (volume in μL)

	HEPES buffer (25 mM, pH8)	Liposomes (1.4 mM total lipid)	MgSO ₄ (2 M in HEPES)	GAG (1 μM in HEPES)
Liposomes only	306	50	---	---
Liposomes + GAG	246	50	---	60
Liposomes + Mg ²⁺	300	50	6	---
Liposomes + Mg ²⁺ + GAG	240	50	6	60

Table 2Preparation of liposome aggregates for saturation tests (all volumes in μL)

	HEPES buffer (25 mM, pH 8)	Liposomes (1.4 mM total lipid)	MgSO ₄ at 2 M	GAG (concentration in parentheses)
Liposomes only + Mg ²⁺	300	50	6	---
100 nM GAG	264	50	6	35.6 (1 μM)
500 nM GAG	122	50	6	178 (1 μM)
1 μM GAG	296	50	6	3.6 (100 μM)
10 μM GAG	264	50	6	35.6 (100 μM)
50 μM GAG	122	50	6	178 (100 μM)
100 μM GAG	264	50	6	35.6 (1 mM)
250 μM GAG	211	50	6	89 (1 mM)
500 μM GAG	122	50	6	178 (1 mM)

Table 3Preparation of liposome aggregates for **170 nM** contamination study (all volumes in μL)

	HEPES buffer (25 mM, pH 8)	Liposomes (1.4 mM total lipid)	MgSO ₄ at 2 M	Heparin (1 μM concentration)	Over-sulfated contaminant
Heparin only	240	50	6	60	--
0.5 mol% contamination	237.3	50	6	59.7	3 (100 nM)
1.0 mol% contamination	234.3	50	6	59.4	6 (100 nM)
2.5 mol% contamination	240	50	6	58.5	1.5 (1 μM)
5.0 mol% contamination	240	50	6	57	3 (1 μM)
10.0 mol% contamination	240	50	6	54	6 (1 μM)
15.0 mol% contamination	240	50	6	51	9 (1 μM)
20.0 mol% contamination	240	50	6	48	12 (1 μM)
30.0 mol% contamination	240	50	6	42	15 (1 μM)

Table 4Preparation of liposome aggregates for **500 nM** contamination study (all volumes in μL)

	HEPES buffer (25 mM, pH 8)	Liposomes (1.4 mM total lipid)	MgSO ₄ at 2 M	Heparin (1 μM concentration)	Over-sulfated contaminant
Heparin only	122	50	6	178	--
0.5 mol% contamination	114	50	6	177.11	8.9 (100 nM)
1.0 mol% contamination	122	50	6	176.2	1.78 (1 μM)
2.5 mol% contamination	122	50	6	173.6	4.45 (1 μM)
5.0 mol% contamination	122	50	6	169.1	8.9 (1 μM)
10.0 mol% contamination	122	50	6	160.2	17.8 (1 μM)
15.0 mol% contamination	122	50	6	151.3	26.7 (1 μM)
20.0 mol% contamination	122	50	6	142.4	35.6 (1 μM)
30.0 mol% contamination	122	50	6	124.6	53.4 (1 μM)

Table 5

Diameters and Zeta potentials of POPC-containing liposomes in the presence of GAG, with and without Mg^{2+} .

Formulation	Zeta potential (mV)	Diameter (nm)
Liposomes only	-13.3 ± 0.78	183.1 ± 8.01
Liposomes + Heparin	-11.6 ± 1.16	177.0 ± 3.94
Liposomes + OSH	-12.1 ± 0.80	174.4 ± 6.35
Liposomes + OSCS	-12.3 ± 0.37	186.8 ± 3.2
Liposomes + OSD	-12.2 ± 0.41	173.5 ± 4.45
Liposomes + Mg^{2+}	4.4 ± 0.61	179.5 ± 1.58
Liposomes + Mg^{2+} + Heparin	4.6 ± 0.58	540.8 ± 50.49
Liposomes + Mg^{2+} + OSH	4.7 ± 0.75	773.9 ± 78.54
Liposomes + Mg^{2+} + OSCS	3.2 ± 0.97	2098.6 ± 192.87
Liposomes + Mg^{2+} + OSD	3.7 ± 0.80	3325.8 ± 543.79

Table 6

Diameters and Zeta potentials of DSPC-containing liposomes in the presence of GAG, with and without Mg^{2+} .

Formulation	Zeta potential (mV)	Diameter (nm)
Liposomes only	-11.8 ± 0.28	254.9 ± 90.97
Liposomes + Heparin	-11.4 ± 0.81	374.2 ± 61.16
Liposomes + OSH	-11.9 ± 0.44	445.9 ± 68.92
Liposomes + OSCS	-11.7 ± 0.43	429.4 ± 36.72
Liposomes + OSD	-12.7 ± 0.34	426.6 ± 58.89
Liposomes + Mg^{2+}	10.3 ± 0.91	397.7 ± 96.19
Liposomes + Mg^{2+} + Heparin	6.7 ± 1.11	2603 ± 189.51
Liposomes + Mg^{2+} + OSH	6.7 ± 1.08	1873 ± 162.66
Liposomes + Mg^{2+} + OSCS	-16.0 ± 0.62	2483 ± 200.76
Liposomes + Mg^{2+} + OSD	-2.7 ± 0.67	3489 ± 762.22

Table 7Heat required for liposome melting (μJ)

GAG	Liposomes only	1 μM	250 μM
Heparin	1709.1	2814.9	2887.1
OSCS	1709.1	3338.2	3367.5
OSD	1709.1	3693.2	2793.5
OSH	1709.1	3653.9	3853.4

Table 8

Molecular Weight of GAGs (g/mol)

GAG	Liposomes only
Heparin	13,500
OSCS	29,560
OSD	42,529